Editors' Suggestion

Metallic Bonding in Close-Packed Structures: Structural Frustration from a Hidden Gauge Symmetry

Eric He,[1,2,*] C. M. Wilson,[2,†] and R. Ganesh[2,‡]
[1]*University of California, Berkeley, California 94720, USA*
[2]*Department of Physics, Brock University, St. Catharines, Ontario L2S 3A1, Canada*

(Received 3 June 2024; revised 16 August 2024; accepted 30 October 2024; published 17 December 2024)

Based on its simple valence electron configuration, we may expect lithium to have straightforward physical properties that are easily explained. However, solid lithium, when cooled below 77 K, develops a complex structure that has been debated for decades. A close parallel is found in sodium below 36 K where the crystal structure still remains unresolved. In this Letter, we explore a possible driving force behind this complexity. We begin with the observation that Li and Na form close-packed structures at low temperatures. We demonstrate a gauge symmetry that forces all close-packed structures to have the same electronic energy and, in fact, the very same band structure. This symmetry requires two conditions: (a) bands must arise from *s* orbitals, and (b) hoppings beyond second-nearest neighbors must be negligible. We argue that both can be reasonably invoked in Li and Na. When these conditions are satisfied, we have extensive degeneracy with the number of competing isoenergetic structures growing exponentially with system size. Weak effects, such as *p*-orbital admixture, long-range hopping, and phonon zero-point energy, can break this symmetry. These can play a decisive role in "selecting" one particular ordered structure. This point of view may explain the occurrence of ordered structures in Li and Na under pressure. Our results suggest that martensitic transitions may also occur in heavier alkali metals such as potassium.

DOI: 10.1103/PhysRevLett.133.256401

Introduction—Systems with extensive degeneracy are fertile ground for interesting physical properties. This is best seen in the field of frustrated magnetism where a large number of classical magnetic orders compete [1,2]. A decisive role is then played by otherwise-small effects such as spin wave entropy, magnon zero-point energy, impurities, etc. [3–5]. They may "select" one particular ordered state or even give rise to liquidlike disordered states [6]. In this Letter, we bring out an analog wherein a large number of crystal structures compete with one another. The competition is among close-packed structures, a family of structures with a long history dating from Kepler's conjecture in 1611 [7,8]. Their realizations include more than half of all elemental solids [9,10]. We argue that they compete and give rise to structural frustration in lithium and sodium.

The low-temperature, ambient-pressure structure of lithium has been debated for decades. At room temperature and pressure, lithium crystallizes in the bcc structure. A martensitic transition occurs when cooled to 77 K, first reported by Barrett in 1947 [11]. Neutron diffraction measurements of McCarthy *et al.* in 1980 revealed that the new phase is neither fcc nor hcp [12]. In 1984, Overhauser proposed the 9*R* structure, a close-packed structure with a nine-layer unit cell [13]. Subsequent neutron experiments found evidence of stacking faults as well as the coexistence of the fcc, hcp, and 9*R* structures at short ranges [14–18]. More recently, in 2017, Elatresh *et al.* [19] argued that de Haas–van Alphen measurements are inconsistent with the 9*R* structure. In the same year, a comprehensive study by Ackland *et al.* [20] concluded that the actual ground state of Li is fcc. A similar picture emerges in sodium, where Barrett demonstrated a martensitic transition below 36 K [21,22]. Despite multiple studies stretching over decades [16,23–27], the structure at lower temperatures remains unresolved.

These studies reveal competition among close-packed structures in Li and Na. This is surprising given that phases such as fcc, hcp, and 9*R* have entirely different symmetries. There is no *a priori* reason for them to be close in energy. We propose an explanation in the form of a hidden gauge symmetry, building upon little known results of Thorpe [28] and Betteridge [29] that point to degeneracies in tight binding bands of close-packed solids.

Close-packed structures and their representations—Close-packed structures are the densest possible arrangements of spheres in three dimensions [30,31], with a packing fraction of ~74%. They are constructed by stacking layers of triangular-lattice arrangements. Each layer must be laterally displaced in one of two directions relative to the layer below. This leads to three possible lateral

---

[*] Contact author: heeric@berkeley.edu
[†] Contact author: cw14mi@brocku.ca
[‡] Contact author: r.ganesh@brocku.ca

positions for each layer, denoted by A, B, C. A close-packed structure can be denoted as a Barlow stacking sequence—a sequence of letters where no two adjacent letters can be the same. For example, fcc is represented as (ABC), a three-letter pattern that repeats indefinitely. The number of close-packed structures grows exponentially with the number of layers. As each layer can take one of two letters (to be distinct from the previous layer), M layers can be stacked in 2^{M-1} ways [32].

The Hägg code [33] is a dual representation that maps each close-packed structure onto a 1D Ising configuration. The Ising variable represents a certain "chirality"—the change of lateral position upon moving along the stacking direction. We define the chirality for $A \to B \to C \to A$ as $+1$, and for $A \to C \to B \to A$ as -1. The fcc structure maps to an Ising ferromagnet, with all chirality variables being $+1$ (or all being -1). Below, we will consider a structure with a repeating M-layer pattern. In the Hägg code, this yields a sequence of M Ising variables with periodic boundaries: σ_j, where $j = 1, \ldots, M$ with $\sigma_{M+1} \equiv \sigma_1$. The "net chirality" defined as $\sum_{j=1}^{M} \sigma_j$ will play a crucial role. We will then discuss the general case with no periodicity in stacking.

Geometry of close packing—We consider a stacking sequence which repeats periodically along the $\hat{\mathbf{z}}$ axis after M layers. The underlying Bravais lattice is hexagonal, with primitive lattice vectors

$$\hat{\boldsymbol{a}} = \hat{\mathbf{x}}, \qquad \hat{\boldsymbol{b}} = R\left(\frac{2\pi}{3}\right)\hat{\mathbf{a}}, \qquad \hat{\boldsymbol{c}} = M\sqrt{\frac{2}{3}}\hat{\mathbf{z}}, \tag{1}$$

where $R(\theta)$ denotes counterclockwise rotation about $\hat{\boldsymbol{c}}$ by angle θ. The spacing between adjacent layers in any closed-packed solid is $\sqrt{\frac{2}{3}}(2r)$, where r is the atomic radius. The units of length in Eq. (1) are chosen such that $2r = 1$. The unit cell contains M basis atoms, one from each layer, with an example shown in Fig. 1.

In any close-packed structure, all atoms have a similar local environment. There are 12 nearest neighbors (1 nn), that can be divided into three sets: (i) Within the same layer, there are six 1nn located at the corners of a hexagon centered at the reference atom as shown in Fig. 2. For later use, we denote the vectors connecting the center of the hexagon to its corners as $\mathcal{N}_{\parallel}$. (ii) Three 1nn are located in the layer above, shown in Fig. 2. Their relative positions belong to one of two possible sets, depending on the chirality between the two layers. We denote these sets as $\mathcal{N}_{\perp}^{+}$ and $\mathcal{N}_{\perp}^{-}$. Each set contains three vectors, with all vectors having the same projection along the stacking direction (same $\hat{z}$ component). (iii) Finally, there are three 1 nn in the layer below.

There are six second-nearest neighbours (2 nn): three in the layer above (see Fig. 2) and three in the layer below. Their positions relative to the reference atom depend on the chirality between the respective layers. We define two sets of 2 nn vectors to the neighbors in the layer above: $\mathcal{N}_{2,\perp}^{+}$ and $\mathcal{N}_{2,\perp}^{-}$.

For third (3 nn) and further neighbors, the environment may differ from one close-packed structure to another. For example, in the hcp structure, there are two 3 nn located at precisely $\pm 2\sqrt{\frac{2}{3}}\hat{\mathbf{z}}$. In the fcc structure, there are no atoms located at these relative positions. Supplemental Material compiles this information in the form of a neighbor table [34].

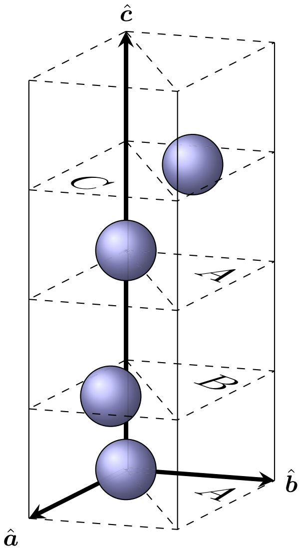

FIG. 1. Hexagonal unit cell of $(ABAC)$ close packing. There are four basis atoms, one from each layer. The basis atom from layer B (C) is located at the centroid of the "up" triangle ("down" triangle).

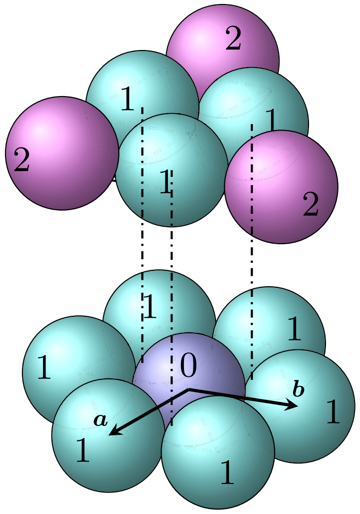

FIG. 2. Local atomic environment in the sequence $\ldots AB \ldots$. Layers are offset in the stacking direction for clarity. The reference atom is labeled "0." Its nearest and second-nearest neighbors are labeled "1" and "2," respectively.

Tight binding description—In the fcc structure, Li and Na have nearly spherical Fermi surfaces arising from a single band with dominant s-orbital character [19,27,35]. In a generic close-packed structure, we describe bands arising from a single s orbital in each atom's valence shell [36]. For simplicity, we proceed assuming that orbitals on distinct atoms are orthogonal to one another. If this assumption is relaxed, the symmetry described below will still hold provided only 1 nn bonds are retained. A detailed discussion is presented in Supplemental Material [34].

Each orbital can be written as $|u,v,w,\alpha\rangle$, where (u,v,w) are integers that pick a unit cell. The index $\alpha \in [1,M]$ picks one atom from the M-atom basis. Assuming electrons can hop to 1 nn and 2 nn, the Hamiltonian acts as follows:

$$\hat{H}|u,v,w,\alpha\rangle = -t \sum_{(u_1,v_1,w_1,\alpha_1)\in 1nn} |u_1,v_1,w_1,\alpha_1\rangle - t' \sum_{(u_2,v_2,w_2,\alpha_2)\in 2nn} |u_2,v_2,w_2,\alpha_2\rangle, \tag{2}$$

where t and t' are hopping amplitudes to 1nn and 2nn, respectively. The accompanying summations are over nearest and next-nearest neighbors of (u,v,w,α). We propose the following Bloch wave ansatz for the stationary states of $\hat{H}$:

$$|\boldsymbol{k}\rangle \propto \sum_{u,v,w}\sum_{\alpha=1}^{M} c_\alpha e^{i\boldsymbol{k}\cdot\boldsymbol{R}_{uvw\alpha}}|u,v,w,\alpha\rangle, \tag{3}$$

where $\boldsymbol{k}$ is the crystal momentum, c_α are coefficients to be determined, and $\boldsymbol{R}_{uvw\alpha}$ is the position vector of the atom (u,v,w,α). Asserting that Eq. (3) is an eigenstate of $\hat{H}$, we are led to diagonalizing the following matrix:

$$H(\boldsymbol{k}) = \begin{pmatrix} V_D & V_1 & 0 & \cdots & V_M^* \\ V_1^* & V_D & V_2 & \ddots & 0 \\ 0 & \ddots & \ddots & \ddots & \vdots \\ \vdots & & V_{M-2}^* & V_D & V_{M-1} \\ V_M & 0 & \cdots & V_{M-1}^* & V_D \end{pmatrix}, \tag{4}$$

where each entry is a function of $\boldsymbol{k}$ (argument suppressed for brevity). The diagonal entries are identical, given by $V_D = V_0 - t\sum_{\boldsymbol{\eta}\in\mathcal{N}_\parallel} e^{i\boldsymbol{k}\cdot\boldsymbol{\eta}}$, where V_0 is the on-site contribution, and the remaining terms arise from hopping to 1 nn within the same layer. The off-diagonal entries depend on chirality variables. Denoting the close-packed structure as $(\sigma_1,\ldots,\sigma_M)$ in Hägg code notation, the right-of-diagonal entry V_j depends on σ_j. It takes two possible values given by

$$V_+ = -t\sum_{\boldsymbol{\eta}\in\mathcal{N}_\perp^+} e^{i\boldsymbol{k}\cdot\boldsymbol{\eta}} - t'\sum_{\boldsymbol{\eta}\in\mathcal{N}_{2,\perp}^+} e^{i\boldsymbol{k}\cdot\boldsymbol{\eta}},$$

$$V_- = -t\sum_{\boldsymbol{\eta}\in\mathcal{N}_\perp^-} e^{i\boldsymbol{k}\cdot\boldsymbol{\eta}} - t'\sum_{\boldsymbol{\eta}\in\mathcal{N}_{2,\perp}^-} e^{i\boldsymbol{k}\cdot\boldsymbol{\eta}}. \tag{5}$$

These terms encode hoppings to the next layer, including 1 nn and 2 nn. Crucially, V_+ and V_- have the same amplitude but may differ in phase; see Supplemental Material [34]. For later use, we write

$$V_+(\boldsymbol{k}) = V_-(\boldsymbol{k})e^{2i\phi(\boldsymbol{k})}, \tag{6}$$

where $\phi(\boldsymbol{k})$ is a $\boldsymbol{k}$-dependent phase. The eigenvalues of Eq. (4) evaluated at each $\boldsymbol{k}$ within the Brillouin zone give the electronic band structure.

Gauge symmetry with periodic boundaries—Consider two distinct close-packed structures denoted as $(\sigma_1,\ldots,\sigma_M)$ and $(\chi_1,\ldots,\chi_M)$ in Hägg code notation. As both have the same number of layers, they share the same primitive lattice vectors as given in Eq. (1) and consequently, the same Brillouin zone. For a given momentum within this Brillouin zone $\boldsymbol{k}$, we define their Bloch Hamiltonians as $H_\sigma(\boldsymbol{k})$ and $H_\chi(\boldsymbol{k})$, both of the form given in Eq. (4). Remarkably, these Hamiltonians are related by a unitary gauge transformation *if* the two configurations have the same net chirality, i.e., if $\sum_j \sigma_j = \sum_j \chi_j$. To demonstrate this, we propose a transformation matrix

$$W_{\sigma,\chi} = \mathrm{diag}(e^{i\theta_1}, e^{i\theta_2},\ldots,e^{i\theta_M}), \tag{7}$$

where $\{\theta_j\}$ are to be determined so as to satisfy

$$W_{\sigma,\chi}^\dagger H_\sigma(\boldsymbol{k}) W_{\sigma,\chi} = H_\chi(\boldsymbol{k}). \tag{8}$$

From the form of the generic Hamiltonian in Eq. (4), we see that the diagonal terms (V_D's) are preserved under the transformation by W. These terms are identical in $H_\sigma(\boldsymbol{k})$ and $H_\chi(\boldsymbol{k})$. We then examine off-diagonal terms. We denote the right-of-diagonal terms in these two Hamiltonians as $V_j(\sigma_j)$ and $V_j(\chi_j)$, respectively. If $\sigma_j = \chi_j$, they are the same. If not, one must be given by V_+ and the other by V_-, both defined in Eq. (5). In order to satisfy Eq. (8), we must have $V_j(\sigma_j)e^{i(\theta_{j+1}-\theta_j)} = V_j(\chi_j)$. This reduces to

$$(\theta_{j+1}-\theta_j) = (\chi_j - \sigma_j)\phi(\boldsymbol{k}), \tag{9}$$

where $\phi(\boldsymbol{k})$ is defined in Eq. (6). These relations determine θ_j's. If Eq. (9) is summed over j's, the left side vanishes due to telescopic cancellation. In order to have consistent θ_j values, the right side must also vanish when summed. This can only happen when $\sum_j \sigma_j = \sum_j \chi_j$. We have arrived at a constraint for when $W_{\sigma,\chi}$ can be chosen to satisfy Eq. (8):

The two close-packed structures must have the same net chirality.

For two close-packed structures that are periodic with the same number of layers and have the same net chirality, the Bloch Hamiltonians at each momentum are unitarily related. It follows that the two structures have precisely the same band structure. When these bands are filled by placing the system in contact with an electron reservoir, the two structures will have the same electronic energy for any chemical potential and temperature. This situation is reminiscent of Ising magnets where the energy only depends on the net magnetization [37]. The configuration space separates into sectors characterized by net chirality, some having large degeneracies. An example with $M = 18$ layers is discussed in Supplemental Material [34].

Gauge symmetry with open boundaries—We now consider open, rather than periodic, boundary conditions along the stacking direction. This choice is more realistic and applies to single-grain crystals grown in experiments. We may use the Hamiltonian matrix of Eq. (4), but with the corner entries V_M and V_M^* set to zero. In this setting, all close-packed structures are degenerate regardless of chirality. Given any pair of structures, we can always construct a transformation matrix of the form in Eq. (7). There are $M - 1$ relations of the form Eq. (9) that constrain M variables (θ_j's); a nontrivial solution always exists.

The symmetry can also be seen from an alternative argument. At each $\boldsymbol{k}$, the band energies are roots of the characteristic equation $\det(H(\boldsymbol{k}) - E) = 0$. Since $H(\boldsymbol{k})$ is tridiagonal, the determinant can be evaluated using transfer matrices [38]:

$$\det(H - E) = \left[\prod_{j=2}^{M} \begin{pmatrix} V_D - E & -|V_j|^2 \\ 1 & 0 \end{pmatrix} \begin{pmatrix} V_D - E & 0 \\ 1 & 0 \end{pmatrix}\right]_{11}.$$

As we have already established, $|V_+|^2 = |V_-|^2$. There is nothing in the matrix product above which depends on the particular stacking sequence. For all M-layer sequences, the eigenenergies are the roots of the same characteristic equation. If these levels are filled, all stacking sequences will have the same energy, irrespective of the chemical potential and temperature. We conclude that all close-packed structures with the same number of layers and open ends are degenerate.

We argue that even with periodic boundaries, energy differences among close-packed structures are subextensive; they do not grow linearly with the number of layers [34]. For example, fcc and hcp differ in energy when periodic boundaries are imposed. However, the energy difference calculated on a per-atom basis vanishes in the thermodynamic limit.

Symmetry breaking effects—We have demonstrated a large ground state degeneracy that emerges from a gauge symmetry. Our arguments are based on standard assumptions in any discussion of band structure, viz., translational symmetry (within layers), the Born-Oppenheimer approximation, negligible interactions, etc. We now explore some effects that could disrupt the gauge symmetry and lead to ordering.

Higher orbitals: Our arguments are based on a tight binding description of s orbitals. With higher orbitals such as p, d, etc., the tridiagonal form of Eq. (4) will still hold (assuming hopping is truncated at second-nearest neighbors). However, the elements of Eq. (4) will be promoted to matrices; e.g., if each atom contributes one s and three p orbitals, we will have 4×4 blocks with entries that can be written systematically using Slater-Koster parameters [39,40]. With multiple entries in each block, a simple gauge transformation of the form Eq. (7) can no longer relate two different Bloch Hamiltonians.

Surprisingly, numerical results indicate that an approximate degeneracy survives when p orbitals are included. In Supplemental Material [34], we discuss the band structure of lithium with $2s$ and $2p$ orbitals included. By systematically tuning p-orbital admixture, we find that close-packed structures develop a spread in energies. However, this spread is comparable to the scale of the martensitic transition. This indicates that a large number of structures compete with one another below the transition.

Phonon zero-point energies: Our arguments are based solely on electronic energy. Standard calculations of phonon band structures using the General Utility Lattice Program [41] do not show any degeneracy among close-packed structures; see Supplemental Material [34]. We consider the $T \to 0$ limit, where phonons can only contribute to energy via a zero-point contribution. We estimate this contribution to be a few percent of the electronic energy [34]. Nevertheless, it may break the degeneracy and select a certain close-packed structure. This could explain the recent observation of fcc order in lithium at low temperatures [20]. In frustrated magnets, it is well known that zero-point energies of spin waves can lead to "state selection" [42,43]. With structural frustration, phonon zero-point energies play an analogous role.

At finite temperatures, phonons bands are occupied according to the Bose-Einstein distribution. They contribute to energy and entropy. Their free energy may break the degeneracy or even favor an entirely different structure; e.g., see Ref. [44]. This could explain the appearance of non-close-packed bcc order above a critical temperature [45].

Long-ranged hopping: The gauge symmetry only applies if hopping beyond second neighbors is negligible. If the solid is pressurized, atoms will move closer and longer-range processes will emerge. This may explain the fact that Li and Na order under pressure [46,47]. To estimate the relevance of long-ranged hopping under ambient pressure, we evaluate a ratio, $\rho = a/a_0$, where a is the experimentally determined lattice constant, and a_0 is the atomic radius. A large value $\rho \gg 1$ indicates that atoms are well separated, and long-ranged hoppings are negligible. We find $\rho_{Li} \sim 2.31$ and $\rho_{Na} \sim 2.26$. As they are greater than unity, it is reasonable to neglect long-ranged hoppings. In fact, heavier alkali metals also have similar values with $\rho_K \sim 2.31$, $\rho_{Rb} \sim 2.24$, and $\rho_{Cs} \sim 2.14$. This suggests that they may also show frustration and a martensitic transition, perhaps requiring lower temperatures and longer annealing than explored previously.

Discussion—Upon cooling, solids typically become more ordered in their structure. In systems that undergo a disordering transition [48,49], the ordered phase is at low temperatures, while the disordered phase appears at high temperatures. Lithium and sodium are two striking counterexamples. They lose order when cooled, with the disordered phase seemingly extending to zero temperature. We provide an explanation in terms of a gauge symmetry that connects an infinite family of idealized close-packed structures.

Our arguments based on a tight binding approach can be compared with the substantive *ab initio* literature on ordering in lithium and sodium [50–54]. Unlike *ab initio* studies which are restricted to small system sizes, our tight binding approach treats all close-packed structures on the same footing. Boundary conditions play an important role; periodic boundaries along the stacking direction artificially limit the degeneracy. An interesting future direction is to examine whether the small energy differences seen in *ab initio* studies are affected by choice of boundary conditions.

Acknowledgments—We thank K. Samokhin for helpful discussions. This work was supported by the Natural Sciences and Engineering Research Council of Canada (NSERC) through Discovery Grant No. 2022-05240. E. H. acknowledges support from NSERC through Undergraduate Student Research Award Grant No. 592911-2024. C. M. W. acknowledges support from NSERC under the Postgraduate Scholarships - Doctoral program (PGS-D Grant No. 581595407).

E. H. and C. M. W. contributed equally to this work.

---

[1] J. T. Chalker, Geometrically frustrated antiferromagnets: Statistical mechanics and dynamics, in *Introduction to Frustrated Magnetism: Materials, Experiments, Theory*, edited by C. Lacroix, P. Mendels, and F. Mila (Springer, Berlin, 2011), pp. 3–22.

[2] A. P. Ramirez, Strongly geometrically frustrated magnets, Annu. Rev. Mater. Res. **24**, 453 (1994).

[3] J. Villain, R. Bidaux, J.-P. Carton, and R. Conte, Order as an effect of disorder, J. Phys. **41**, 1263 (1980).

[4] C. L. Henley, Ordering due to disorder in a frustrated vector antiferromagnet, Phys. Rev. Lett. **62**, 2056 (1989).

[5] E. F. Shender and P. C. W. Holdsworth, Order by disorder and topology in frustrated magnetic systems, in *Fluctuations and Order: The New Synthesis*, edited by M. Millonas (Springer, New York, 1996), pp. 259–279.

[6] L. Balents, Spin liquids in frustrated magnets, Nature (London) **464**, 199 (2010).

[7] J. Kepler, *The Six-Cornered Snowflake* (Clarendon Press, Oxford, 1966).

[8] G. Szpiro, *Kepler's Conjecture* (John Wiley, New York, 2003).

[9] W. Steurer, Crystal structures of the elements, in *Encyclopedia of Materials: Science and Technology*, edited by K. J. Buschow, R. W. Cahn, M. C. Flemings, B. Ilschner, E. J. Kramer, S. Mahajan, and P. Veyssière (Elsevier, Oxford, 2001), pp. 1880–1897.

[10] J. Arblaster, *Selected Values of the Crystallographic Properties of the Elements* (ASM International, Materials Park, OH, 2018).

[11] C. S. Barrett, A low temperature transformation in lithium, Phys. Rev. **72**, 245 (1947).

[12] C. M. McCarthy, C. W. Tompson, and S. A. Werner, Anharmonicity and the low-temperature phase in lithium metal, Phys. Rev. B **22**, 574 (1980).

[13] A. W. Overhauser, Crystal structure of lithium at 4.2 K, Phys. Rev. Lett. **53**, 64 (1984).

[14] R. Berliner and S. Werner, The structure of the low temperature phase of lithium metal, Physica (Amsterdam) **136B+C**, 481 (1986).

[15] H. G. Smith, Martensitic phase transformation of single-crystal lithium from bcc to a 9*R*-related structure, Phys. Rev. Lett. **58**, 1228 (1987).

[16] R. Berliner, O. Fajen, H. G. Smith, and R. L. Hitterman, Neutron powder-diffraction studies of lithium, sodium, and potassium metal, Phys. Rev. B **40**, 12086 (1989).

[17] H. Smith, R. Berliner, and J. Jorgensen, Martensitic transformation from BCC to 9*R* and FCC in metallic lithium, Physica (Amsterdam) **156-157B**, 53 (1989).

[18] W. Schwarz and O. Blaschko, Polytype structures of lithium at low temperatures, Phys. Rev. Lett. **65**, 3144 (1990).

[19] S. F. Elatresh, W. Cai, N. W. Ashcroft, R. Hoffmann, S. Deemyad, and S. A. Bonev, Evidence from Fermi surface analysis for the low-temperature structure of lithium, Proc. Natl. Acad. Sci. U.S.A. **114**, 5389 (2017).

[20] G. J. Ackland, M. Dunuwille, M. Martinez-Canales, I. Loa, R. Zhang, S. Sinogeikin, W. Cai, and S. Deemyad, Quantum and isotope effects in lithium metal, Science **356**, 1254 (2017).

[21] C. S. Barrett, Metallographic study of sodium, potassium, rubidium, and caesium after cooling to 1.2° K, J. Inst. Met. **84**, 43 (1955).

[22] C. S. Barrett, X-ray study of the alkali metals at low temperatures, Acta Crystallogr. **9**, 671 (1956).

[23] D. L. Martin, Thermal effects of the martensitic transition in sodium, Phys. Rev. Lett. **1**, 4 (1958).

[24] D. Hull and H. M. Rosenberg, Microscopy at liquid helium temperatures: Phase transition in sodium, Phys. Rev. Lett. **2**, 205 (1959).

[25] J. Szente and J. Trivisonno, Ultrasonic study of the martensitic phase transformation in sodium, Phys. Rev. B **37**, 8447 (1988).

[26] R. Berliner, H. G. Smith, J. R. D. Copley, and J. Trivisonno, Structures of sodium metal, Phys. Rev. B **46**, 14436 (1992).

[27] S. F. Elatresh, M. T. Hossain, T. Bhowmick, A. D. Grockowiak, W. Cai, W. A. Coniglio, S. W. Tozer, N. W. Ashcroft, S. A. Bonev, S. Deemyad, and R. Hoffmann, Fermi surface studies of the low-temperature structure of sodium, Phys. Rev. B **101**, 220103(R) (2020).

[28] M. F. Thorpe, Random walks in polytype structures, J. Math. Phys. (N.Y.) **13**, 294 (1972).

[29] G. P. Betteridge, Compaison of the s band structure of face centred cubic and hexagonal close packed solids. The common zone approach, Phys. Status Solidi (b) **107**, 791 (1981).

[30] P. Krishna and D. Pandey, *Close-packed structures* (International Union of Crystallography, Cardiff, 1981).

[31] J. Conway, E. Bannai, N. Sloane, J. Leech, S. Norton, A. Odlyzko, R. Parker, L. Queen, and B. Venkov, *Sphere Packings, Lattices and Groups*, Grundlehren der mathematischen Wissenschaften (Springer, New York, 2013).

[32] R. M. Thompson and R. T. Downs, Systematic generation of all nonequivalent closest-packed stacking sequences of length *N* using group theory, Acta Crystallogr. Sect. B **58**, 153(E) (2002).

[33] G. Hägg, Some notes on MX_2 layer lattices with close-packed X atoms, Arkiv foer Kemi, Mineralogi och Geologi **16B**, 1 (1943).

[34] See Supplemental Material at http://link.aps.org/supplemental/10.1103/PhysRevLett.133.256401 for a table of nearest-neighbor distances, details of the tight-binding setup, subextensive energy differences with periodic boundaries, phonon band structures, and various symmetry-breaking effects.

[35] T. Bhowmick, S. F. Elatresh, A. D. Grockowiak, W. Coniglio, M. T. Hossain, E. J. Nicol, S. W. Tozer, S. A. Bonev, and S. Deemyad, Structure and pressure dependence of the Fermi surface of lithium, Phys. Rev. B **106**, L041112 (2022).

[36] M. P. Marder, Nearly free and tightly bound electrons, in *Condensed Matter Physics* (John Wiley & Sons, Ltd., New York, 2010), Chap. 8, pp. 207–232.

[37] C. Kittel and H. Kroemer, *Thermal Physics* (W. H. Freeman and Company, San Francisco, 1980), Chap. 1.

[38] L. G. Molinari, Determinants of block tridiagonal matrices, Linear Algebra Appl. **429**, 2221 (2008).

[39] J. C. Slater and G. F. Koster, Simplified LCAO method for the periodic potential problem, Phys. Rev. **94**, 1498 (1954).

[40] D. A. Papaconstantopoulos, *Handbook of the Band Structure of Elemental Solids*, 2nd ed. (Springer, New York, 2014).

[41] J. D. Gale and A. L. Rohl, The general utility lattice program (GULP), Mol. Simul. **29**, 291 (2003).

[42] J. G. Rau, P. A. McClarty, and R. Moessner, Pseudo-Goldstone gaps and order-by-quantum disorder in frustrated magnets, Phys. Rev. Lett. **121**, 237201 (2018).

[43] S. Khatua, S. Srinivasan, and R. Ganesh, State selection in frustrated magnets, Phys. Rev. B **103**, 174412 (2021).

[44] L. V. Woodcock, Entropy difference between the face-centred cubic and hexagonal close-packed crystal structures, Nature (London) **385**, 141 (1997).

[45] D. L. Martin and N. F. Mott, The specific heat of lithium from 20 to 300 °K: The martensitic transformation, Proc. R. Soc. A **254**, 444 (1960).

[46] V. G. Vaks, M. I. Katsnelson, V. G. Koreshkov, A. I. Likhtenstein, O. E. Parfenov, V. F. Skok, V. A. Sukhoparov, A. V. Trefilov, and A. A. Chernyshov, An experimental and theoretical study of martensitic phase transitions in Li and Na under pressure, J. Phys. Condens. Matter **1**, 5319 (1989).

[47] A. M. Schaeffer, W. Cai, E. Olejnik, J. J. Molaison, S. Sinogeikin, A. M. dos Santos, and S. Deemyad, Boundaries for martensitic transition of ^{7}Li under pressure, Nat. Commun. **6**, 8030 (2015).

[48] F. C. Nix and W. Shockley, Order-disorder transformations in alloys, Rev. Mod. Phys. **10**, 1 (1938).

[49] É. V. Kozlov, Order-disorder transition and stability of ordered state, Sov. Phys. J. **19**, 1034 (1976).

[50] W. Maysenhölder, S. G. Louie, and M. L. Cohen, Cohesive properties of bcc and fcc rubidium from *ab initio* pseudopotentials, Phys. Rev. B **31**, 1817 (1985).

[51] M. M. Dacorogna and M. L. Cohen, First-principles study of the structural properties of alkali metals, Phys. Rev. B **34**, 4996 (1986).

[52] H. Sankaran, S. M. Sharma, and S. K. Sikka, The low-temperature phase of sodium: An intermediate orthorhombic distortion?, J. Phys. Condens. Matter **4**, L61 (1992).

[53] M. Hutcheon and R. Needs, Structural and vibrational properties of lithium under ambient conditions within density functional theory, Phys. Rev. B **99**, 014111 (2019).

[54] A. Raju Natarajan and A. Van der Ven, Toward an understanding of deformation mechanisms in metallic lithium and sodium from first-principles, Chem. Mater. **31**, 8222 (2019).